Visualization of Dark Side of Skull Base with Surgical Navigation and Endoscopic Assistance: Extended Petrous Rhomboid and Rhomboid with Maxillary Nerve–Mandibular Nerve Vidian Corridor

Kentaro Watanabe[1,2], Ali R. Zomorodi[3], Moujahed Labidi[1], Shunsuke Satoh[3,4], Sébastien Froelich[1], Takanori Fukushima[2]

■ BACKGROUND: **Lesions located at the petrous apex, cavernous sinus, clivus, medial aspect of the jugular foramen, or condylar regions are still difficult to fully expose using the operating microscope. Although approaches to this region through the middle cranial fossa have been previously described, these approaches afford only limited visualization. We have confirmed a transcranial infratemporal fossa combined microsurgical and endoscopic access to the petrous apex, clivus, medial aspect of the jugular foramen, and occipital condyle. We have presented the results of a micro-anatomical cadaver dissection study and its clinical application.**

■ METHODS: **Ten latex-injected cadaveric specimens (20 twenty sides) underwent dissection with navigational guidance to achieve an extended anterior petrosal approach combined with a far vidian corridor approach (between the foramen rotundum and foramen ovale). We performed anatomical dissections to confirm the surgical anatomy and the feasibility and limitations of this approach. Anatomical dissections were performed in the skull base laboratory of Lariboisière Hospital and Duke University Medical Center. This approach was then applied to some clinical cases.**

■ RESULTS: **The combination of the microscope and endoscope, aided by surgical navigation, was extremely effective and provided a wide view of the petrous rhomboid, the entire clivus, and the medial condylar regions. The extended extradural anterior petrosal approach provided a large corridor to petrous and clival lesions. Endoscopic assistance allows for wide and deep exposure of the middle to lower clivus, epipharyngeal space, and bilateral condylar regions. This approach successfully provided adequate surgical access for resection of tumors located in these regions. The depth of the medial aspect of the jugular foramen was 16.3 ± 1.2 mm deep from the geniculate ganglion. The emerging point of the inferior petrosal sinus in the jugular foramen was 16.5 ± 1.8 mm deep from the geniculate ganglion. The hypoglossal canal was 21.6 ± 2.2 mm deep from the geniculate ganglion. The foramen magnum was located 31.5 ± 2.4 mm deep from the gasserian ganglion. The inferior petrosal sinus was found to be a reliable landmark to identify the medial portion of the jugular bulb. The introduction of the endoscope through the middle fossa rhomboid enabled visualization of the medial aspect of the jugular bulb, which otherwise would be hampered by the internal auditory canal under the microscope.**

■ CONCLUSION: **After microscopic exposure of the middle fossa rhomboid, neuronavigational endoscopic assistance facilitated visualization of the ventral cavernous region, petrous apex, retropharyngeal space, and middle and inferior clivus down to the medial aspect of the jugular bulb and condyle regions. Additional maxillary nerve–mandibular nerve vidian corridor visualization provides a lateral transsphenoidal approach to upper clivus lesions.**

Key words
- Clivus
- Condyle
- Endoscopic assistance
- Extended anterior petrosal approach
- Hypoglossal
- Jugular foramen
- Middle fossa approach

Abbreviations and Acronyms
CSF: Cerebrospinal fluid
GPN: Greater petrosal nerve
IAC: Internal auditory canal
ICA: Internal carotid artery
IPS: Inferior petrosal sinus
MRI: Magnetic resonance imaging
SPS: Superior petrosal sinus
V2: Maxillary nerve
V3: Mandibular nerve

From the [1]Department of Neurosurgery, Lariboisière Hospital, Paris VII-Diderot University, Paris, France; [2]Department of Neurosurgery, Tokyo Jikei University school of Medicine, Tokyo, Japan; [3]Division of Neurosurgery, Duke University Medical Center, Durham, North Carolina, USA; and [4]Department of Neurosurgery, Southern Tohoku General Hospital, Koriyama-shi, Japan

To whom correspondence should be addressed: Kentaro Watanabe, M.D. [E-mail: kentarow31@gmail.com]

*Citation: World Neurosurg. (2019) 129:e134-e145.
https://doi.org/10.1016/j.wneu.2019.05.062*

*Journal homepage: **www.journals.elsevier.com/world-neurosurgery***

*Available online: **www.sciencedirect.com***

INTRODUCTION

During the previous 30 years, skull base surgeons have developed extended skull base techniques to access difficult anatomic areas.[1] Even with these techniques, and with advanced microscopic visualization, some areas of the skull base, such as the ventral cavernous sinus, petrous apex, clivus, and the medial aspect of the jugular bulb and condylar regions, have remained hidden to the microscope. Recently, transnasal approaches through the sphenoid and maxillary sinuses and transpterygoid and/or transclivus approaches have been used successfully to treat medial jugular lesions and lower clivus condylar lesions. Despite these developments, we have sometimes still realized a benefit from the use of transcranial approaches because these do not share some of the limitations of even extended endoscopic exposures (e.g., lesions that extend above and below the lateral cavernous sinus).

During the past 5 years, our group has been aiming to visualize these hidden areas using high-resolution 4-mm, rigid endoscopic techniques with transcranial approaches. We have found a unique benefit in anatomical visualization by combining these techniques with our previously described extended skull base approaches. In the present report, we have described a navigational endoscopic study using cadaveric head specimens and clinical applications, focusing on the extended anterior petrosal approach.

The purpose of the present study was to perform a morphometric analysis of the extended middle fossa rhomboid and an additional maxillary nerve (V2)-mandibular nerve (V3) vidian corridor to the middle and lower clivus around the medial jugular bulb and condyle using cadaveric head models (Figures 1 and 2) and to report our clinical experience with these approaches.

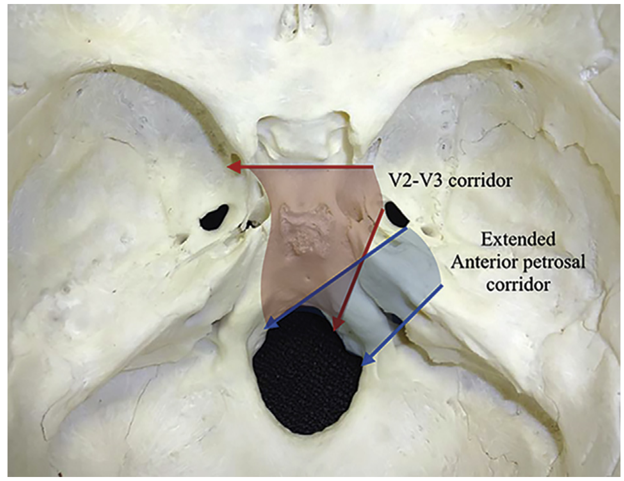

Figure 1. Superior view of the skull base with directions of the vidian corridor (*red*) and extended anterior petrosal approach (*blue*). V2, maxillary nerve; V3, mandibular nerve.

METHODS

Ten fixed cadaveric heads had been dissected with a microscope (OPMI Pico [Carl Zeiss, Inc., Oberkochen, Germany]) and endoscope (Karl Storz GmbH, Tuttlingen, Germany) and used for photography. For the endoscopic approaches, we used an 18-cm-long, 4-mm in diameter endoscope with a 0°, 30°, and 70° lens. Endoscopic images were recorded and stored using the Karl Storz Aida system (Karl Storz GmbH). Measurement of the exposure thus obtained was performed with a surgical navigation system (Medtronic, Minneapolis, Minnesota, USA). Microsurgical cadaveric dissections were performed to achieve an extended anterior petrosal approach, a combined anterior petrosal approach, and the V2-V3 vidian corridor approach. The anatomical dissections were performed at the anatomical laboratory for skull base surgery at Duke University Hospital and Lariboisière Hospital.

Positioning and Surgical Technique

The head was fixed in a Mayfield head holder (Integra LifeSciences, Plainsboro, New Jersey, USA) and turned 70° with 5° of extension. The posterior border of the temporal muscle was incised and detached from the temporal bone using the retrograde dissection technique to protect the deep temporal nerve and arteries by the temporal muscle fascia. A 5-cm × 5-cm craniotomy was performed, and the middle fossa was accessed extradurally. The foramen spinosum was identified, following the middle meningeal artery, and was coagulated and cut. The foramen ovale and foramen rotundum were also identified. A small incision of the dura mater above the foramen ovale was made, and the dura propria was elevated. Dissection over the greater petrosal nerve (GPN) was performed from posteriorly to anteriorly to protect the nerve. The arcuate eminence and GPN and petrous ridge were exposed completely. The rhomboid area (Kawase triangle with postmeatal area)[2-8] defined by the posterior border of the V3, GPN, arcuate eminence, and petrous ridge were exposed.

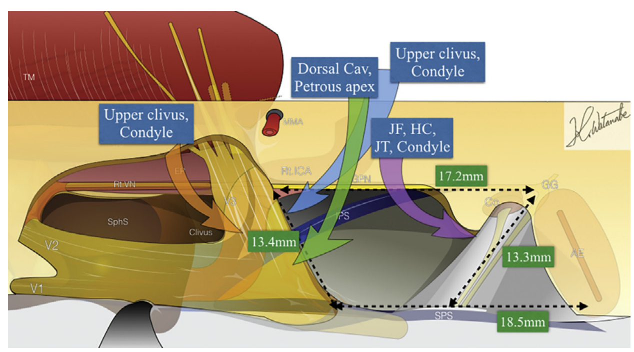

Figure 2. Schematic representation the infratemporal fossa, with opening of the maxillary nerve—mandibular nerve corridor and petrous rhomboid. The *blue arrow* shows the direction of access to the upper, middle, and lower clivus through the vidian corridor. The *green arrow* shows the trajectory to the petrous apex and inferior cavernous sinus through the petrous rhomboid. The *purple arrow* shows the posterior view to the medial jugular foramen and hypoglossal canal through the petrous rhomboid. Cav, cavity; AE, arcuate eminence; Co, cochlear; IPS, inferior petrosal sinus; GG, genicurate ganglion; GPN, greater petrosal nerve; MMA, middle meningeal artery; SphS, sphenoid sinus; SPS, superior petrosal sinus; HC, hypoglossal canal; JF, jugular foramen; JT, jugular tubercle; SphS, sphenoid sinus.

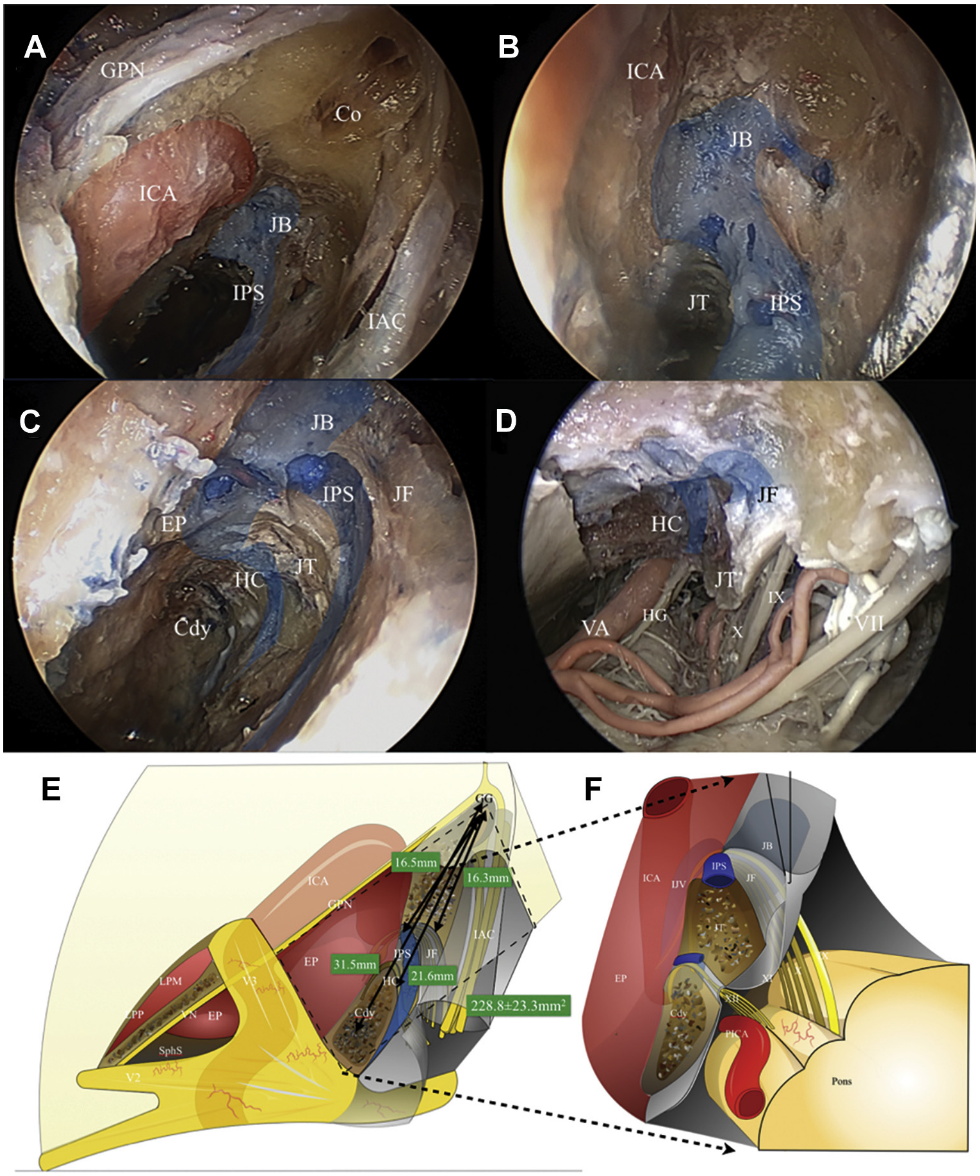

Figure 3. (**A**) Endoscopic view, in a posterior trajectory, through the petrous rhomboid. The inferior petrosal sinus (IPS), which connects to the medial wall of the jugular bulb (JB), is visualized below the cochlea (Co). (**B**) The horizontal segment of the internal carotid artery (ICA) was skeletonized and followed posteriorly to the vertical segment of the ICA, close to the jugular bulb. (**C**) The IPS was cut, exposing the medial wall of the jugular foramen (JF). The jugular tubercle (JT) is located between the jugular foramen and hypoglossal canal (HC). Under the hypoglossal canal, the condyle and foramen magnum can be accessed. (**D**) The dura mater of the posterior fossa was opened. The cranial nerves VII, VIII, IX, X, XI, and XII and vertebral artery (VA) can be identified in the intradural space. (**E,F**) Schematic drawing showing a posterior view onto the medial part of the jugular foramen through the petrous rhomboid. GPN, greater petrosal nerve.

Next, through the rhomboid, an anterior petrosectomy was achieved toward the petrous apex and ventral cavernous sinus wall. The petrous bone was drilled from the petrous apex anteriorly to the anterior border of the superior semicircular canal posteriorly. The dura of the internal auditory canal (IAC) was completely exposed. Inferiorly, the inferior petrosal sinus (IPS) could be exposed on the inferior petrosal sinus groove. Normally, the IPS is a landmark of the inferior limit of petrous bone removal. When the tumor extends to the clivus and/or condyle, the tumor will provide a tumor corridor across the IPS. The IPS leads to the medial aspect of the jugular bulb and location of the jugular complex. A partial clivectomy could be

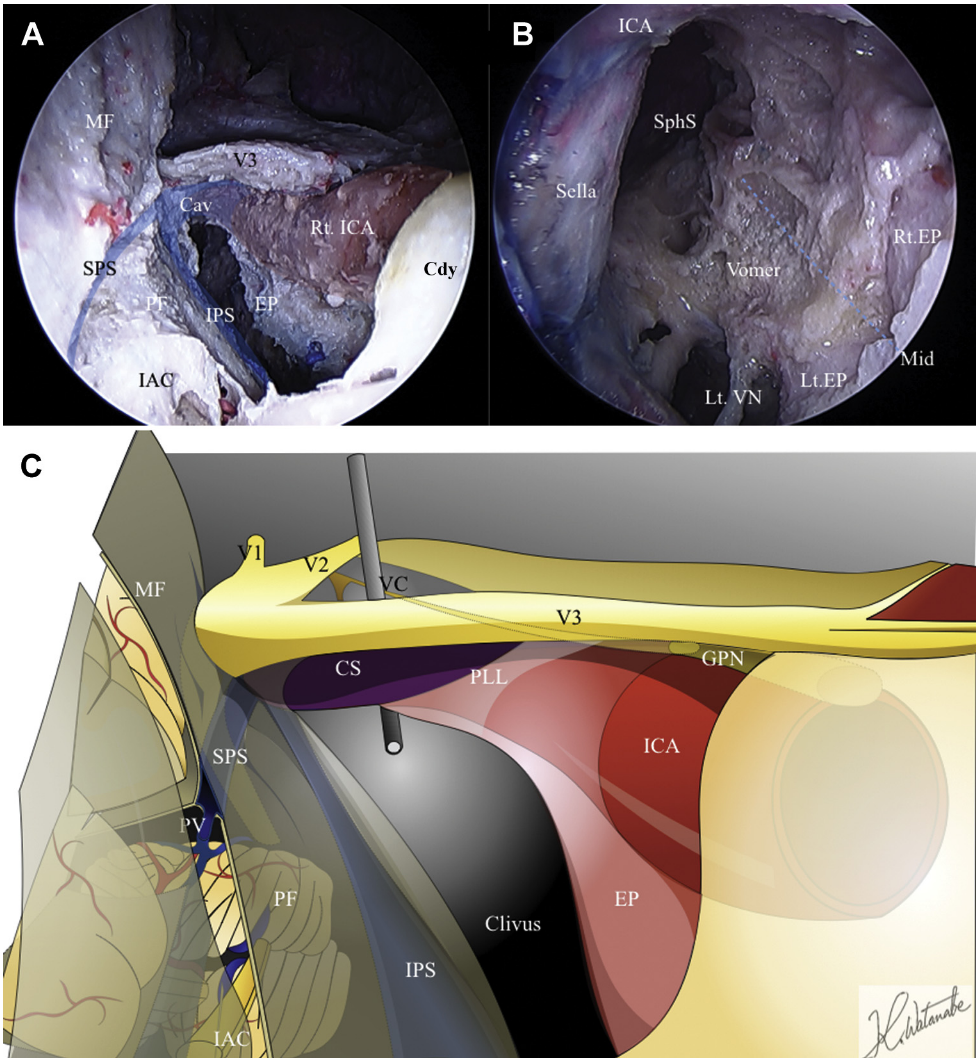

Figure 4. Cadaveric endoscopic images and schema of the anterior view from the anterior petrosal approach. (**A**) Endoscopic anterior view through the petrous rhomboid corridor after removing the petrous apex and upper clival bone. The internal carotid artery (ICA) goes into the cavernous sinus. The superior petrosal sinus (SPS) and inferior petrosal sinus (IPS) emerge from the cavernous sinus. (**B**) Inside view into the sphenoid sinus (SphS) from the petrous rhomboid. Upper clival bone was partially drilling and the dura of clivus was exposed posteriorly and the epipharynx wall was exposed anteriorly. (**C**) Schematic drawing showing anterior view through the anterior petrosal corridor with endoscopic illumination of the maxillary nerve—mandibular nerve (V2-V3) corridor. Cdy, condyle; EP, epipharynx; HC, hypoglossal canal; JT, jugular tubecle; JF, jugular foramen; Lt, left; MF, middle fossa; Mid, midline; Mid DM, middle fossa dura mater; ON, optic nerve; Rt, right; VC, vidian corridor; VN, vidian nerve.

performed by removing the bone around the jugular foramen (Figure 3). To visualize the area below the IAC, endoscopic-assisted visualization is necessary.

To continue to remove the clivus and condyle below the IPS, the addition of the V2-V3 corridor will help with visualization and lighting. The V2-V3 vidian corridor, defined as the space between the V2 and V3 and medial to the vidian nerve, was exposed in the far lateral triangle.[9,10] The bone located in the V2-V3 vidian corridor, which is the pterygoid process (or root of the pterygoid) was drilled until the epipharynx was reached inferiorly and the sphenoid sinus medially (Figure 2).

Working through the V2-V3 vidian corridor, navigational-assisted endoscopic examination of the posterior clinoid and dorsum sella, petrous apex, ventral cavernous sinus, and contralateral condylar space was performed. This maneuver was performed on 20 sides of 10 fixed human cadaveric heads and was then performed in 26 clinical cases without, and 4 cases with, endoscope assistance.

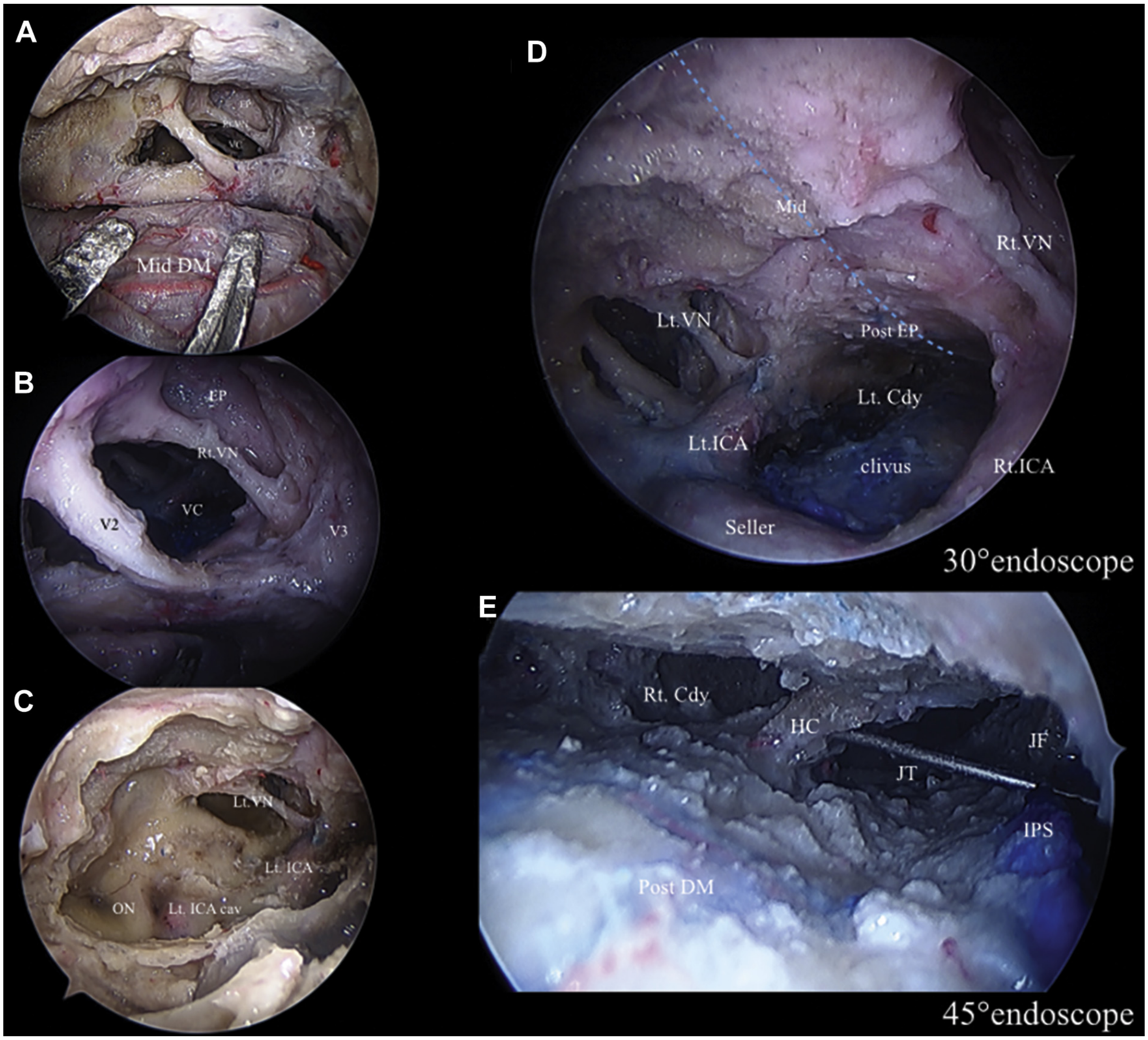

Figure 5. Cadaveric images of the maxillary nerve—mandibular nerve (V2-V3) corridor. (**A**) Infratemporal fossa view with exposure of V2, V3, and root of the pterygoid, which was completely drilled. The V2-V3 corridor was opened with complete exposure of the right vidian nerve. (**B**) Entrance of the vidian corridor into the sphenoid sinus between the right vidian nerve and V2. (**C**) View inside the sphenoid sinus. The contralateral vidian nerve, internal carotid artery, and optic nerve can be seen. (**D**) Inferior view from the vidian corridor after drilling of the clivus. The posterior fossa dura mater of the clivus and posterior wall of the epipharynx were exposed. (**E**) Endoscopic view (45°) of the clivus. The jugular foramen, hypoglossal canal, and condyle can be seen. A cannula was inserted through the petrous rhomboid corridor.

RESULTS

An extended extradural anterior petrosal approach provides a view along the surgical trajectory from the middle fossa to the medial aspect of the jugular foramen and condyle region inferiorly. The IPS can be followed to the medial aspect of the jugular foramen and condyle. Between the pharyngeal wall and posterior fossa dura, the bone corridor provides a narrow, but usable, extradural corridor for clivus removal. The inferior extension of petrous rhomboid drilling can provide exposure of the medial condyle complex up to the level of the hypoglossal canal. Laterally and anteriorly, the posterior wall of the retropharyngeal mucosa was found behind the internal carotid artery (ICA). Inferiorly and posteriorly, the middle and lower clivus were exposed up to the level of the foramen magnum. Also, additional bone removal of the root of pterygoid through the V2-V3 vidian corridor (**Figure 2**) allows for an access route to the upper and middle clivus posteroinferiorly. The space left by drilling in the V2-V3 vidian corridor can be used to insert the endoscope and achieve visualization into the sphenoid sinus and sphenoclival junction. Dorsally, the V2-V3 vidian corridor leads to the upper lateral

Table 1. Transcranial Surgical Cases of Middle Fossa Tumors

Pt. No.	Age (years)	Sex	Pathological Entity	Location	Resection (Remaining Region)	Approach	Neurological Deficit
1	72	M	Chondrosarcoma	Pet, CL	STR, (CL, Cdy)	APA	
2	59	M	GSPN schwannoma	Pet, Pterygoid	GTR	APA	
3	53	M	Hemangioma	Pet, CL	PR (CL, JB)	2-Stage; APA	
4	28	M	Chordoma	CS	STR	APA	
5	59	M	Chordoma	Pet	GTR	APA	
6	29	M	Chordoma	Pet, CS	PR (BS)	APA	VII
7	55	M	Chordoma	Pet, CS, CL, Cdy	STR (BS, CL, Cdy)	APA + Trans CS	V, VIII
8	57	F	Chordoma	Pet, CS,	STR (CS)	APA + Trans CS	
9	48	M	Chondrosarcoma	Pet, CS, JB	STR (CS, CL, Cdy)	APA + V2-V3	Preoperative (VI, IX, X, XII)
10	57	F	Chordoma	Pet	GTR	APA	
11	70	F	Chordoma	Pet	GTR	APA	
12	37	M	Chordoma	Pet, CS	GTR	APA + Trans CS	VI
13	52	F	Chordoma	Pet, JB	GTR	APA	
14	47	F	Chordoma	Pet, JB	STR (CL)	APA	IX
15	35	M	Chondrosarcoma	Pet	GTR	APA	
16	29	M	Vidian schwannoma	Sph, Pet	STR (CS)	APA + V2-V3	Dry eye
17	47	M	Chondrosarcoma	Pet	GTR	APA	
18	42	F	Chordoma	Pet, CS	GTR	APA + V2-V3, endoscope	
19	37	M	Chordoma	Pet, CS, CL, Cdy	GTR	APA, endoscope	
20	51	M	Chondrosarcoma	Pet, CS, CL	STR (CS)	APA + V2-V3, endoscope	
21	73	M	Chondrosarcoma	Pet	GTR	APA, endoscope	

Pt. No., patient number; M, male; Pet, petrosal bone; STR, subtotal resection; CL, clivus; Cdy, condyle; APA, anterior petrosal approach; GSPN, greater superficial petrosal nerve; GTR, gross total resection; PR, partial resection; JB, jugular bulb; CS, cavernous sinus; BS, brain stem; F, female; Sph, sphenoid sinus; V2, trigeminal second branch; V3, trigeminal nerve third branch.

epipharynx wall. Posteroinferiorly, at the level of the middle and lower clivus, it follows to the posterior wall of the epipharynx.

Morphometric Analysis

Middle Fossa Rhomboid. The GPN length from its exit from the geniculate ganglion to its entrance point under the trigeminal nerve was found to be, on average, 17.2 ± 3.8 mm. The mean IAC length from the geniculate ganglion to the petrous ridge was 13.3 ± 0.8 mm. The petrous ridge length from the IAC's anterior dural limit to the trigeminal nerve posterior edge was 18.5 ± 1.5 mm, on average. The mean posterior edge length of the trigeminal nerve (V3) from the GPN to the petrous edge was 13.4 ± 2.6 mm. The average rhomboid area in the specimens studied was 228.8 ± 23.3 mm^2. Anterior translocation of the trigeminal nerve by 5 mm provided additional space of 69.9 ± 7.1 mm^2, with a maximal surface of 297.6 ± 30.4 mm^2 (Figure 3E).

Posterior View From Rhomboid Corridor. *Jugular Foramen and Hypoglossal Canal in lateral Clivus From Petrous Rhomboid.* The IPS's emergence from the jugular bulb was, on average, 16.3 ± 1.2 mm deep from the geniculate ganglion. The superior aspect of the ninth cranial nerve was 16.5 ± 1.8 mm deep from the geniculate ganglion, on average (Figure 3E). The IPS originates from the posterior cavernous sinus and tracks down in the posterior fossa dura toward the jugular bulb (Figure 3A,B,E). Below the 9th and 10th cranial nerve complex, the hypoglossal canal is found (Figure 3C). The hypoglossal canal is located 21.6 ± 2.2 mm deep from the geniculate ganglion (Figure 3E). The distance between the inferior edge of the clivus and the midpoint of the GPN was 31.5 ± 2.4 mm, on average. This approach was also found to reach the contralateral lower clivus at the level of the foramen magnum.

Posteroinferior Deep View From Rhomboid Corridor. *Intradural Anatomical Structures and Relationship of Jugular Foramen and Hypoglossal Canal.* The endoscopic view of the medial wall of the jugular foramen and condylar region through the middle fossa rhomboid is shown in Figure 3. The 9th and 10th cranial nerves can be seen at their origin from the postolivary sulcus of the upper medulla and hypoglossal nerve at its exit from the medulla in the preolivary sulcus (Figure 3D,E). Drilling of the petrous bone, followed by drilling of the medial jugular region and condyle, allowed for exposure of the IPS in its entire length. After cutting the IPS and opening the dura of the posterior

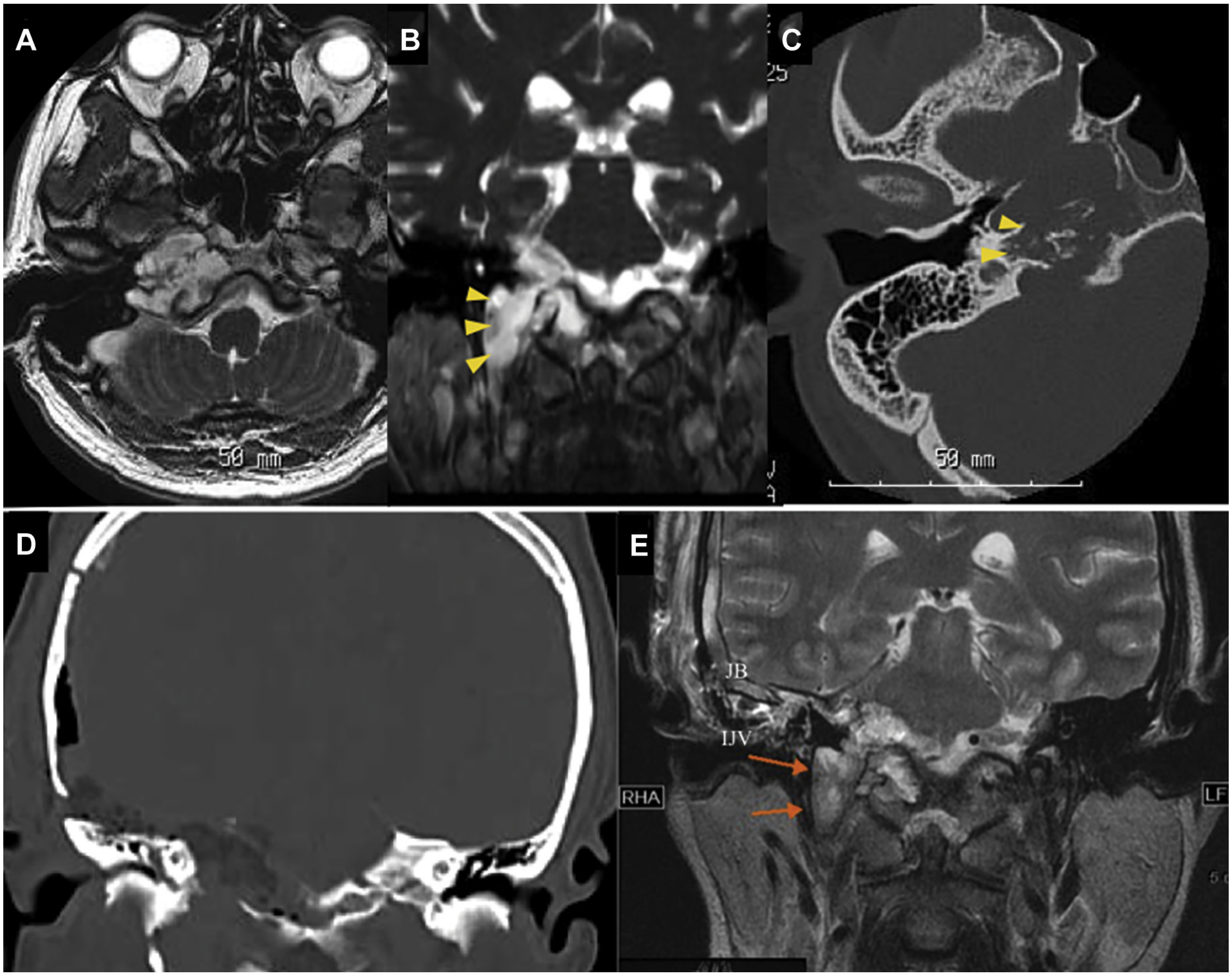

Figure 6. (**A**) Axial T2-weighted magnetic resonance image showing a lesion in the petrous bone, extending medially to the jugular foramen. (**B**) Coronal T2-weighted magnetic resonance image showing tumor extension at the level of C1. The *yellow arrow heads* show the tumor extends the level of the C1. (**C**) Computed tomography image showing the osteolysis in the petrous bone. The *yellow arrow heads* show the tumor invade into the petrous bone. (**D**) Postoperative computed tomography scan showing an anterior petrosal corridor reaching down to the level of C1. (**E**) Postoperative T2-weighted magnetic resonance image showing tumor was removed down to the level of the jugular bulb and internal jugular vein. *Orange arrows* show the cavity where the tumor was removed.

fossa, a downward view on the lateral pons and medulla can be obtained.

Anterior View From Rhomboid Corridor. The petrous apex and upper clivus can be removed under visualization with the endoscope. The inferior wall of the cavernous sinus superiorly, posterior fossa dura mater medially, and ICA petrous segment and epipharyngeal superior wall laterally can be exposed (Figure 4). The IPS is a landmark for the junction between the petrous bone and the clivus. The sphenoid sinus and vidian corridors can be connected (Figure 5) and used to visualize the upper clivus (Figure 5B) and middle and lower clivus until the ipsilateral and contralateral condyle (Figure 5D,E).

V2-V3 Corridor to Clivus. The vidian nerve was found at a mean depth of 8.0 ± 1.2 mm below and parallel to the V2 through the space between the V2 and V3. This corridor leads to the region of the ventral cavernous sinus to the mid-inferior clivus posteriorly. The direction of the V2-V3 corridor posteroinferiorly is aimed at the lower clivus and contralateral condyle, between the posterior constrictor muscle of the posterior wall of the epipharynx and posterior fossa dura mater (Figure 2). The contralateral lower clivus at the level of the foramen magnum can also be exposed

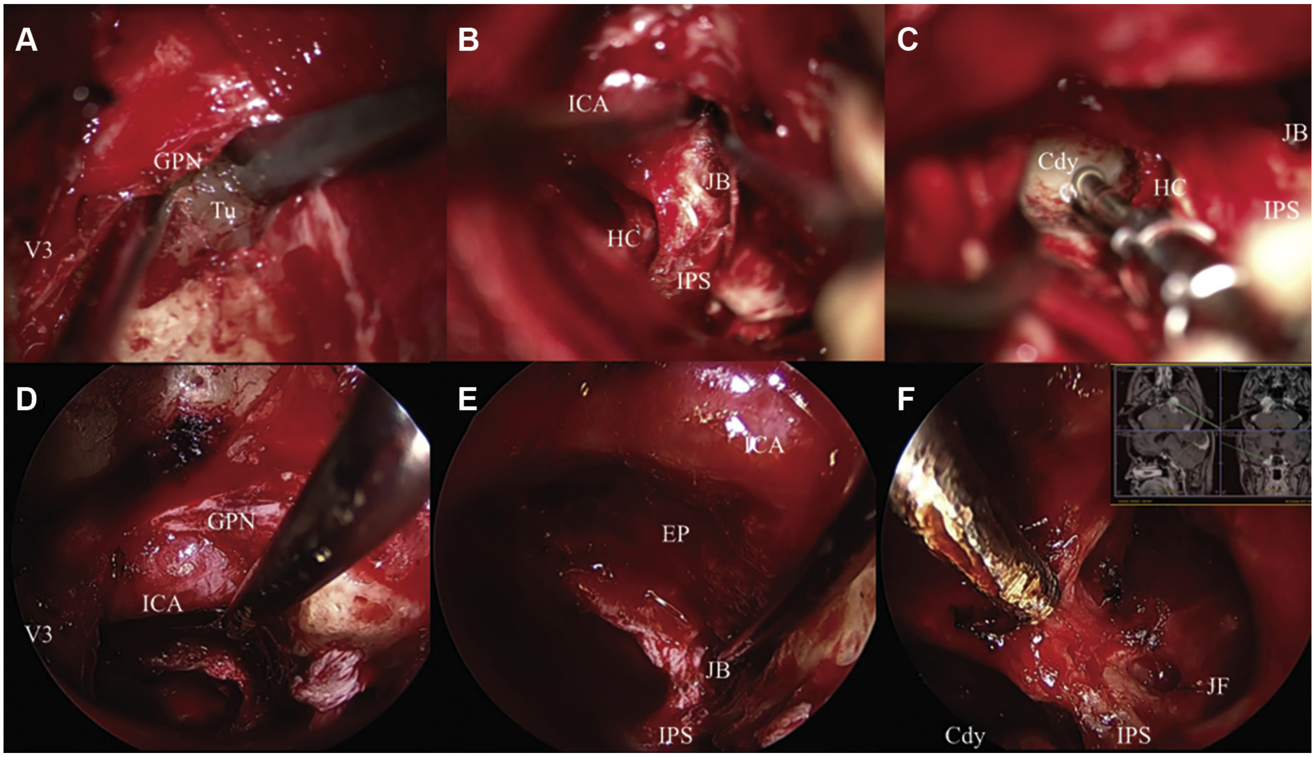

Figure 7. (**A**) Intraoperative microscopic image showing the tumor located below the greater petrosal nerve (GPN). Mandibular nerve (V3) was transposed anteriorly. (**B**) After removing the tumor, the inferior petrosal sinus (IPS) indicates the location of the jugular bulb (JB). The hypoglossal canal (HC) can be seen under the IPS. (**C**) The tumor infiltration into the condyle (Cdy) was removed. (**D**) Intraoperative endoscopic view through the petrous rhomboid. (**E**) Below the internal carotid artery (ICA), the posterior wall of the epipharyngeal mucosa was exposed, and the IPS and JB were identified. (**F**) Posterior view with a 30° endoscope visualizing the tumor located in the jugular foramen (JF). The tumor extending into the jugular foramen was removed under endoscopic visualization.

by adjusting the angle of the surgical trajectory (Figure 5). Endoscopic assistance can be used to visualize the structures and pathologic features inside and through the sphenoid sinus and also to visualize the contralateral vidian nerve.

Clinical Illustration

Before the development of endoscopic surgery, we approached the middle fossa, petrous, and extended cavernous sinus tumors through the anterior petrosal approach. In our clinical data, we identified 18 patients who had been treated via the anterior petrosal approach without endoscopic assistance. (Table 1) In addition, 4 patients were identified who had undergone surgery via the anterior petrosal approach with endoscopic assistance.

Patient 1: Extended Middle Fossa Rhomboid with Endoscopic Assistance. A 37-year-old patient, who had initially presented with hearing disturbance and facial weakness, underwent magnetic resonance imaging (MRI). The MRI scan revealed a large lesion in the petrous apex, extending to the lower clivus and C1 condyle (Figure 6). Tumor extension into the intradural space was also suspected. The preoperative presumptive diagnosis was chordoma, and we elected to proceed through an extended anterior petrosal approach. The tumor was soft and was removed mostly by aspiration under microscope guidance. We identified the IPS and medial wall of the jugular bulb, and followed the tumor until the hypoglossal canal was exposed (Figure 7). The condyle was drilled to remove the tumor-invaded bone. Next, the endoscope provided additional visualization of the medial wall of the jugular foramen and inferior aspect of the hypoglossal canal, which will be hidden from microscopic view by the IAC and hypoglossal canal (Figure 7D–F). Also, the tumor compartment, which extended intradurally was removed under endoscopic view through the petrous rhomboid. A postoperative MRI scan demonstrated gross total resection of the tumor (Figure 6E,F). The histopathological examination showed chondroid chordoma.

Patient 2. Combined Extended Rhomboid with V2-V3 Vidian Corridor Approach. The second patient was a 51-year-old man who had presented with nasal congestion. The MRI scan demonstrated a large tumor located in the infratemporal and clival region. Extensive petrous and clivus bone erosion and invasion into the cavernous sinus were present (Figure 8A–D). Most of the tumor was removed under microscopic visualization from the rhomboid and vidian corridors. The ICA was already occluded and was resected (Figure 8E). The endoscope improved the

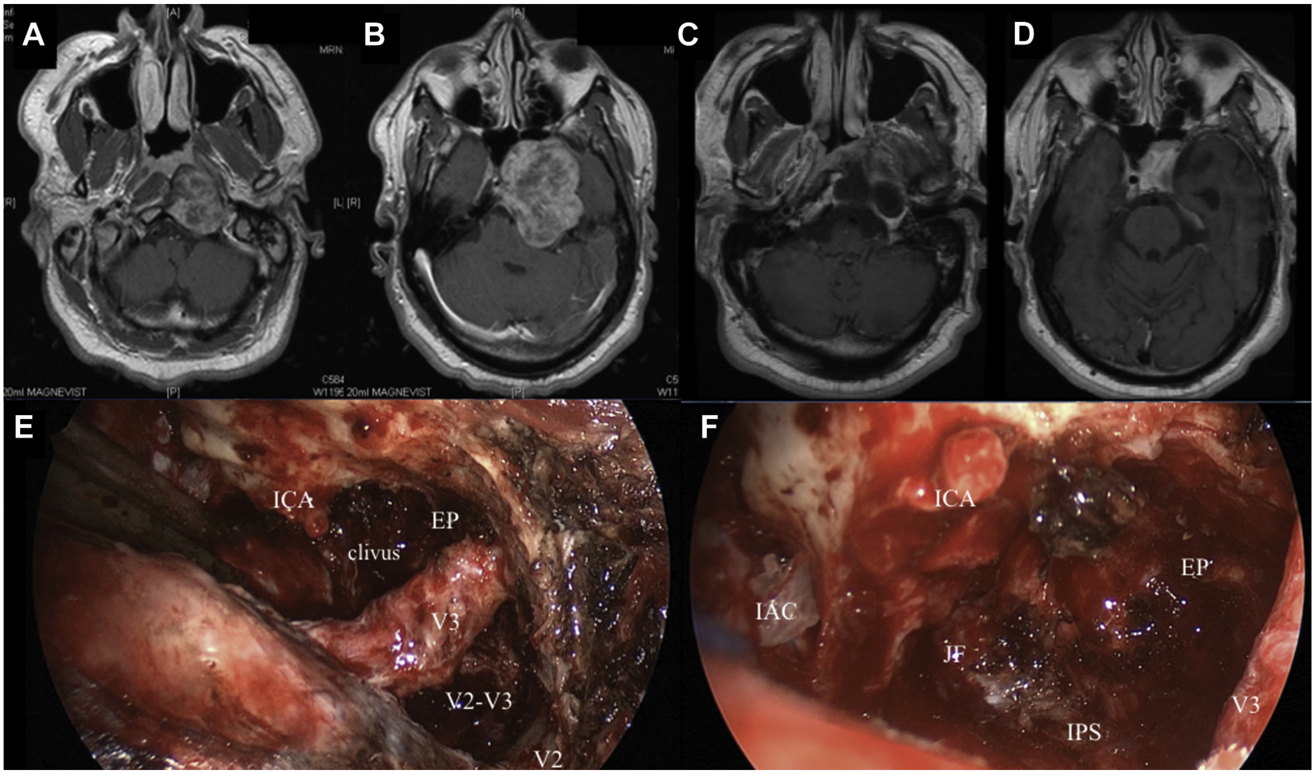

Figure 8. (**A,B**) T1-weighted, gadolinium-enhanced magnetic resonance image demonstrating a large mass effect of the infratemporal fossa. The tumor extended into the posterior pharyngeal space at the level of the hypoglossal canal (HC). The tumor showed displacement of the sphenoid sinus anteriorly and extended into the posterior and middle fossae. No intradural extension was present. (**C,D**) Postoperative T1-weighted gadolinium-enhanced magnetic resonance image showing the middle fossa tumor had been removed. A small piece of tumor remained in the sphenoid sinus. (**E**) The infratemporal fossa was exposed, and most of the tumor had been with microscope guidance. The maxillary nerve (V2) and mandibular nerve (V3) were exposed, and the petrous rhomboid and vidian corridor were opened. The internal carotid artery (ICA) was already occluded and was cut. (**F**) Endoscopic visualization provided a view below V3 and the medial jugular foramen.

working view under the trigeminal nerve in the areas of the petrous apex, inferior wall of cavernous sinus, and middle to lower clivus (**Figure 8F**). Also, the tumor compartment located in the medial jugular and medial condyle region, below the IAC, came well into endoscopic view and was completely resected. The postoperative course was uneventful, with no new cranial nerve deficits. The combination of the vidian triangle and extended rhomboid approach was, thus, useful in patient 2, with endoscopic assistance providing a better downward view on the parts of the tumor not seen with the microscope. The histopathological examination showed chondroid tumor.

Patient 3. Extended Middle Fossa Rhomboid Case. A 73-year-old male patient presented with right abducens nerve palsy. The MRI study showed a mass located in the right petrous apex and extending toward the carotid canal in the petrous bone and inferiorly in the upper clivus (**Figure 9A–C**). Extended anterior petrosectomy was performed with endoscope assistance. After exposure of the GPN, petrous ridge, and lateral wall of the cavernous sinus, including V3 (**Figure 9D**), the posterior border of the V3 was dissected and transposed ∼5 mm anteriorly. Anterior petrosectomy was performed, and the tumor was identified. The petrous bone was drilled to its apex, next to Dorello's canal, and where the IPS emerges from the cavernous sinus inferiorly. Also, the petrous segment of the carotid artery was exposed and followed until its entrance in the cavernous sinus at the petrolingual ligament (inferior wall of the cavernous sinus; **Figure 9E**). The view is similar to the anatomical dissection shown in **Figure 5A**. The tumor, which extended into the petrous carotid canal and upper clivus, was seen under visualization of the endoscope and removed using suction and angled curettes (**Figure 9F**). The histopathological finding was chondrosarcoma.

DISCUSSION

Although many skull base techniques and approaches have been developed to achieve access to the central skull base,[11-16] the exposure provided by traditional open techniques remains quite limited in the area of the lower and lateral clivus.[17] In the past decade, the endoscopic endonasal approach has been developed as a new and rational "workhorse" corridor to access certain lesions located in the midline skull base.[18-24] The reach of the endonasal approach has been rapidly expanded to allow for more

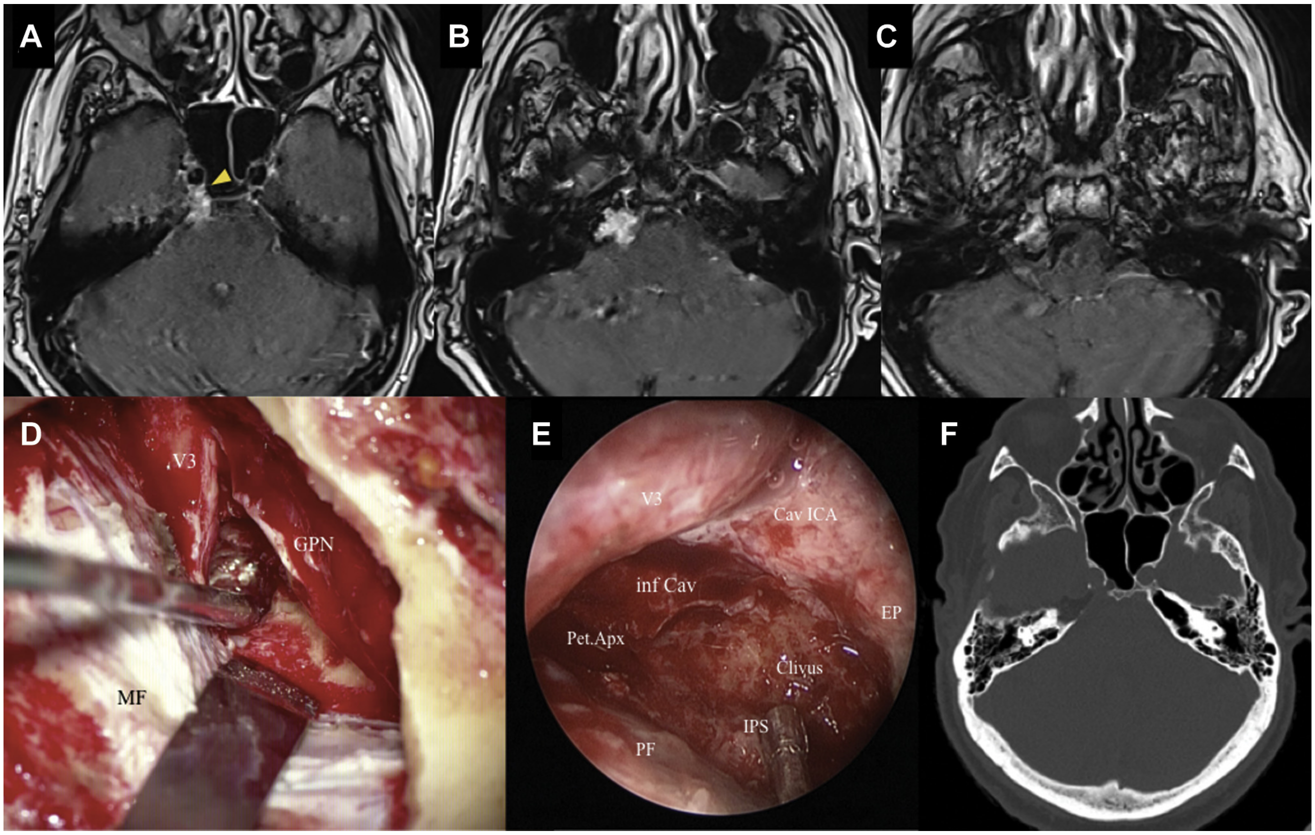

Figure 9. (**A**–**C**) T1-weighted gadolinium-enhanced magnetic resonance image demonstrating a small mass in the petrous apex extending dorsally to the internal carotid artery (ICA) and medially to the jugular foramen. (**D**) Mandibular nerve (V3) was translocated anteriorly, widening the access to the tumor in the petrous bone. (**E**) Endoscopic view below V3. The petrous apex, which had been invaded by the tumor, was removed up to the dura of Dorello's canal and the inferior petrosal sinus (IPS). The cavernous segment of the ICA can be identified under V3. (**F**) Postoperative computed tomography scan showing an anterior petrosal corridor reaching to the petrous apex lesion.

direct access to deep and hidden skull base areas, such as the medial aspect of the clival bone and foramen magnum.[23] Surgical access to the infratemporal fossa and pterygopalatine fossa lesions can also be achieved through an endoscopic endonasal approach.[25] However, some major issues remain associated with the endonasal route, including the loss of quality of life related to mucosal trauma, the risks of cerebrospinal fluid (CSF) leak,[26] and ICA injury or infection.[27] In the case of intradural extension of the resection, the closure will be challenging, requiring complex reconstruction with resulting morbidity (nasoseptal flap),[25] with a reported rate of postoperative CSF leak ranging from 5% to 20%. Although most sinonasal complaints will be transient and will resolve within months, symptoms can persist longer after more complex surgeries and when the mucosal trauma has been more extensive.

Similarly, several studies have explored the role of endoscopic-assisted microsurgery through either a conventional craniotomy or a "keyhole" craniotomy.[22,28,29] In this paradigm shift, investigators have tried to combine the different sets of advantages associated with these 2 modalities.[28]

Extended transnasal approaches are most useful in lesions located in the midline and paramedian skull base. However, for recurrent cases or small tumor remnants, which are located in lateral or deep regions, a lateral transcranial approach might be required. Multiple previous operations will sometimes mandate the use of a new corridor to reduce the risk of neurological morbidity or CSF leakage. Skull base surgeons should have several options to approach these deep regions and should prefer the corridor that allows for the greatest complication avoidance and minimal invasiveness each time.

The classic middle fossa technique is a mature and controllable technique. Endoscopic assistance and navigational assistance provide wide visualization of the hidden area and show the safety corridor for classic open surgery. Hasanbelliu et al.[30] compared the transcranial middle fossa approach and the transsphenoidal–transclival approach to the ventral portion of the pons. They reported that the extended middle fossa approach provided an adequate corridor to lesions in the upper ventrolateral pons. The extended endonasal corridor is better suited for lesions in the midline but is limited when the approach must be extended laterally, beyond the sixth cranial nerve or the foramen lacerum segment of the ICA.

The V2-V3 corridor is a safe pathway to reach lesions located ventral to the cavernous sinus and sphenoid sinus. In the present study, we have shown that the V2-V3 corridor can provide wide and comfortable access to the bilateral lower clivus. Through the sphenoid sinus, and with the aid of endoscopic assistance, the contralateral vidian nerve and ICA can also be accessed.

This combined transcranial extended anterior petrosectomy and additional V2-V3 corridor is useful and does not require the sacrifice of any normal structures, except for the additional extradural bone work. In cases of chordomas or chondrosarcomas, this extradural work and additional bone removal will actually be desirable from a tumor control standpoint, in addition to improving visualization.[18,31,32]

To gain access to the medial inferior clivus and medial condyle, previous reports have described the use of the endonasal approach to the hypoglossal canal and medial aspect of the jugular foramen.[33] We have used this route for many lower clival and upper cervical cases, especially for n primary bony lesions, including chordomas and chondrosarcomas.[34]

The sphenoid sinus provides enough working space for the endoscope, although it requires significant dissection and resection of normal structures. In particular, when exposing the region of the medial aspect of the jugular foramen, condyle dissection and, sometimes, resection of the Eustachian tube can be required. The Eustachian tube opens into the pharyngeal space and is located just under the sphenoclival junction. Its resection can cause chronic serous otitis and pain that can negatively affect patients' quality of life. Simal-Julian et al.[35] reported a technique in which they transposed and preserved the Eustachian tube using an endoscopic endonasal extreme far-medial approach. This could be another option; however, it is not always possible, and exposure will be limited laterally when the Eustachian tube has been preserved. The transnasal transsphenoidal approach has also been used to access lesions of the petrous apex.[36-38] In this corridor, the main element to consider is the exact location and trajectory of the ICA at its paraclival and lacerum segments.[36] The risk of ICA injury is not insignificant with this approach because ICA transposition will sometimes be required to improve visualization in the petrous region.[36,39]

Approach Selection

The most important point in approach selection is concordance between the tumor plane and surgical axis. Anterior petrosectomy follows an oblique axis, which is neither horizontal nor vertical. Thus, in a tumor extending from the middle fossa down to the craniocervical junction area, anterior petrosectomy can provide a reasonable surgical corridor on the condition that the axis of the tumor is congruous. In contrast, when a tumor extends in the anteroposterior plane, the transnasal endoscopic approach will be preferred if the lateral limits of the tumor can be reached.

When a tumor of the petrous apex has both lateral and anterior extensions, an anterior petrosectomy will usually be insufficient because it will be limited by the petrous ICA, V3, and cavernous sinus. Opening the V2-V3 corridor will helps to gain additional exposure anteriorly and laterally.

Complications Avoidance

The most important disadvantages and complications of the infratemporal fossa approach are temporal swelling and contusion, ICA injury, IPS bleeding, CSF leak, and trigeminal nerve injury. In our clinical cases, the temporal lobes were found to be intact on the postoperative imaging studies in all cases. IPS bleeding and cavernous sinus bleeding from the rhomboid approach can be more troublesome and should be thought out in advance. At least 1 of the 2 petrosal sinuses should be preserved. In the case of tumor invasion of the IPS, we take care to preserve a patent superior petrosal sinus (SPS). However, in most cases, the IPS will be larger than the SPS, and hemostasis will be more difficult to achieve if it has been violated.

Just as with the standard middle fossa approach, the petrous ICA can also be injured in the area under V3. Three-dimensional computed tomography angiography and computed tomography venous angiography have been recommended to prepare for this approach. The surgical navigation system is a valuable tool to identify these structures. CSF leakage is also a concern in this corridor, and closure of the posterior fossa dura can be challenging. We recommend using a free fat graft and a vascularized pericranial and fascial flap to close the dura.

CONCLUSION

The corridor developed from the combination of the rhomboid and vidian triangles is potentially a valuable option when resecting lesions located inferiorly to the cavernous sinus and in the medial inferior clivus. The combination of endoscopic and microscopic techniques provides several possibilities. The use of surgical navigational can be helpful in identifying anatomical landmarks such as the IPS, jugular foramen, hypoglossal canal, and so forth. However, a precise understanding of the 3-dimensional surgical anatomy related to this approach is crucial. Skull base neurosurgeons must remain flexible when they devise their surgical strategies and be able to offer the surgical approach most suited for each lesion, whether endoscopic endonasal, conventional and advanced microscopic, and combined endoscopic and microscopic approaches.

REFERENCES

1. Day JD, Fukushima T, Giannotta SL. Microanatomical study of the extradural middle fossa approach to the petroclival and posterior cavernous sinus region: description of the rhomboid construct. *Neurosurgery*. 1994;34:1009-1016 [discussion: 1016].

2. Fukushima T, Day JD, Hirahara K. Extradural total petrous apex resection with trigeminal translocation for improved exposure of the posterior cavernous sinus and petroclival region. *Skull Base Surg*. 1996;6:95-103.

3. Kawase T, Shiobara R, Toya S. Anterior transpetrosal-transtentorial approach for sphenopetroclival meningiomas: surgical method and results in 10 patients. *Neurosurgery*. 1991;28: 869-875 [discussion: 875-876].

4. Kawase T, Toya S, Shiobara R, Mine T. Transpetrosal approach for aneurysms of the lower basilar artery. *J Neurosurg*. 1985;63:857-861.

5. Kawase T, Shiobara R, Toya S. Middle fossa transpetrosal-transtentorial approaches for petroclival meningiomas: selective pyramid resection and radicality. *Acta Neurochir (Wien)*. 1994;129:113-120.

6. Aristegui M, Cokkeser Y, Saleh E, et al. Surgical anatomy of the extended middle cranial fossa approach. *Skull Base Surg*. 1994;4:181-188.

7. Borghei-Razavi H, Tomio R, Fereshtehnejad SM, et al. Anterior petrosal approach: the safety of Kawase triangle as an anatomical landmark for anterior petrosectomy in petroclival meningiomas. *Clin Neurol Neurosurg*. 2015;139:282-287.

8. Maina R, Ducati A, Lanzino G. The middle cranial fossa: morphometric study and surgical considerations. *Skull Base*. 2007;17:395-403.

9. Wanibuchi M, Friedman AH, Fukushima T. *Photo Atlas of Skull Base Dissection: Techniques and Operative Approaches*. New York: Thieme; 2009.

10. Yasuda A, Campero A, Martins C, Rhoton AL Jr, de Oliveira E, Ribas GC. Microsurgical anatomy and approaches to the cavernous sinus. *Neurosurgery*. 2008;62(suppl 3):1240-1263.

11. Goel A. Extended middle fossa approach for petroclival lesions. *Acta Neurochir (Wien)*. 1995;135:78-83.

12. Goel A. Middle fossa sub-Gasserian ganglion approach to clivus chordomas. *Acta Neurochir (Wien)*. 1995;136:212-216.

13. Harsh GR, Sekhar LN. The subtemporal, transcavernous, anterior transpetrosal approach to the upper brain stem and clivus. *J Neurosurg*. 1992;77:709-717.

14. House WF, Gardner G, Hughes RL. Middle cranial fossa approach to acoustic tumor surgery. *Arch Otolaryngol*. 1968;88:631-641.

15. House WF, Hitselberger WE, Horn KL. The middle fossa transpetrous approach to the anterior-superior cerebellopontine angle. *Am J Otol*. 1986;7:1-4.

16. Pensak ML, Van Loveren H, Tew JM Jr, Keith RW. Transpetrosal access to meningiomas juxtaposing the temporal bone. *Laryngoscope*. 1994;104:814-820.

17. Suslu HT, Gayretli O, Coskun O, Bozbuga M, Serifoglu L, Gurses IA. Anatomical and morphometrical evaluation of the jugular tubercle. *Br J Neurosurg*. 2014;28:503-506.

18. Dehdashti AR, Karabatsou K, Ganna A, Witterick I, Gentili F. Expanded endoscopic endonasal approach for treatment of clival chordomas: early results in 12 patients. *Neurosurgery*. 2008;63:299-307 [discussion: 307-309].

19. Fraser JF, Nyquist GG, Moore N, Anand VK, Schwartz TH. Endoscopic endonasal transclival resection of chordomas: operative technique, clinical outcome, and review of the literature. *J Neurosurg*. 2010;112:1061-1069.

20. Fatemi N, Dusick JR, Gorgulho AA, et al. Endonasal microscopic removal of clival chordomas. *Surg Neurol*. 2008;69:331-338.

21. Jho HD, Carrau RL. Endoscopic endonasal transsphenoidal surgery: experience with 50 patients. *J Neurosurg*. 1997;87:44-51.

22. Komatsu F, Komatsu M, Di Ieva A, Tschabitscher M. Endoscopic far-lateral approach to the posterolateral craniovertebral junction: an anatomical study. *Neurosurg Rev*. 2013;36:239-247 [discussion: 247].

23. Morera VA, Fernandez-Miranda JC, Prevedello DM, et al. "Far-medial" expanded endonasal approach to the inferior third of the clivus: the transcondylar and transjugular tubercle approaches. *Neurosurgery*. 2010;66(6 suppl operative):211-219 [discussion: 219-220].

24. Pirris SM, Pollack IF, Snyderman CH, et al. Corridor surgery: the current paradigm for skull base surgery. *Childs Nerv Syst*. 2007;23:377-384.

25. Zanation AM, Snyderman CH, Carrau RL, Gardner PA, Prevedello DM, Kassam AB. Endoscopic endonasal surgery for petrous apex lesions. *Laryngoscope*. 2009;119:19-25.

26. Hong Jiang W, Ping Zhao S, Hai Xie Z, Zhang H, Zhang J, Yun Xiao J. Endoscopic resection of chordomas in different clival regions. *Acta Otolaryngol*. 2009;129:71-83.

27. Maira G, Pallini R, Anile C, et al. Surgical treatment of clival chordomas: the transsphenoidal approach revisited. *J Neurosurg*. 1996;85:784-792.

28. Komatsu F, Komatsu M, Di Ieva A, Tschabitscher M. Endoscopic extradural subtemporal approach to lateral and central skull base: a cadaveric study. *World Neurosurg*. 2013;80:591-597.

29. Komotar RJ, Starke RM, Raper DM, Anand VK, Schwartz TH. The endoscope-assisted ventral approach compared with open microscope-assisted surgery for clival chordomas. *World Neurosurg*. 2011;76:318-327 [discussion: 259-362].

30. Hasanbelliu A, Andaluz NO, Di Somma A, et al. 220 Expanded anterior petrosectomy through the transcranial middle fossa and extended endoscopic transphenoidal-transclival approaches: qualitative and quantitative anatomic analysis. *Neurosurgery*. 2016;63(suppl 1):186.

31. Saito K, Toda M, Tomita T, Ogawa K, Yoshida K. Surgical results of an endoscopic endonasal approach for clival chordomas. *Acta Neurochir (Wien)*. 2012;154:879-886.

32. Stippler M, Gardner PA, Snyderman CH, Carrau RL, Prevedello DM, Kassam AB. Endoscopic endonasal approach for clival chordomas. *Neurosurgery*. 2009;64:268-277 [discussion: 277-278].

33. Benet A, Prevedello DM, Carrau RL, et al. Comparative analysis of the transcranial "far lateral" and endoscopic endonasal "far medial" approaches: surgical anatomy and clinical illustration. *World Neurosurg*. 2014;81:385-396.

34. George B, Bresson D, Bouazza S, et al. [Chordoma]. *Neurochirurgie*. 2014;60:63-140.

35. Simal-Julian JA, Miranda-Lloret P, Beltran-Giner A, Plaza-Ramirez E, Botella-Asuncion C. Full endoscopic endonasal extreme far-medial approach: Eustachian tube transposition. *J Neurosurg Pediatr*. 2013;11:584-590.

36. Van Gompel JJ, Alikhani P, Tabor MH, et al. Anterior inferior petrosectomy: defining the role of endonasal endoscopic techniques for petrous apex approaches. *J Neurosurg*. 2014;120:1321-1325.

37. Muto J, Prevedello DM, Ditzel Filho LF, et al. Comparative analysis of the anterior transpetrosal approach with the endoscopic endonasal approach to the petroclival region. *J Neurosurg*. 2016;125:1171-1186.

38. Feng K, Qiuhang Z, Wei Z, et al. Anatomy of the petrous apex as related to the endoscopic endonasal approach. *J Clin Neurosci*. 2012;19:1695-1698.

39. Mortini P, Mandelli C, Gerevini S, Giovanelli M. Exposure of the petrous segment of the internal carotid artery through the extradural subtempdoral middle cranial fossa approach: a systematic anatomical study. *Skull Base*. 2001;11:177-187.

Conflict of interest statement: The authors declare that the article content was composed in the absence of any commercial or financial relationships that could be construed as a potential conflict of interest.

Received 9 February 2019; accepted 7 May 2019

Citation: World Neurosurg. (2019) 129:e134-e145.
https://doi.org/10.1016/j.wneu.2019.05.062

*Journal homepage: **www.journals.elsevier.com/world-neurosurgery***

*Available online: **www.sciencedirect.com***